Azino-Fused Benzimidazolium Salts as DNA Intercalating Agents. 2.

Joaquín Pastor,[†] Jorge G. Siro,[†] José L. García-Navío,[†] Juan J. Vaquero,[†] Julio Alvarez-Builla,*[,†] Federico Gago,[§] Beatriz de Pascual-Teresa,[§] Manuel Pastor,[§] and M. Melia Rodrigo[‡]

Departamento de Química Orgánica, Departamento de Química-Física, and Departamento de Farmacología, Universidad de Alcalá, 28871 Alcalá de Henares, Madrid, Spain

Received November 4, 1996[⊗]

The synthesis of new pyrido[1,2-*a*]- and pyridazino[1,6-*a*]benzimidazolium salts by basic condensation of 1,3-disubstituted 2-alkylbenzimidazolium salts and 1,2-diketones and subsequent chemical transformations is described. The DNA-binding properties were examined by UV-vis spectroscopy, viscosimetric determinations, and molecular modeling techniques. The presence of a flat polycyclic hydrocarbon moiety such as a naphthalene-1,8-diyl or a biphenyl-*o*,*o*'-diyl, fused to the cationic heterocycle, appears to enhance the interaction with DNA. Variation of the substituents on the indole-like N will allow us to build up a new series of bis-salts with bis-intercalating properties.

Introduction

The DNA molecule is the primary target of many antitumor agents. Among the binding modes of drugs to DNA, both intercalative and nonintercalative mechanisms have been described, and in both cases a certain degree of sequence selectivity has been shown.[1] Intercalators contain a planar chromophore with two to four fused aromatic rings. A positive charge is generally needed for activity.[2] The cationic moiety is usually provided by a quaternized aromatic nitrogen of the chromophore[3a] which can be generated either by simple protonation as in the aminoacridine series (*e.g.* proflavine **1**), or by nucleophilic substitution as found in the well known phenanthridine series (*e.g.* ethidium bromide **2**). Alternatively, it is possible to have a chromophore with the cationic nitrogen shared between two aromatic rings, though to our knowledge there are only two precedents[3b] of this, the indolo[1,2-*a*]quinolizinium alkaloid Sempervirine **3**[4] and the imidazodiquinolinium cation **4**[5] (Figure 1).

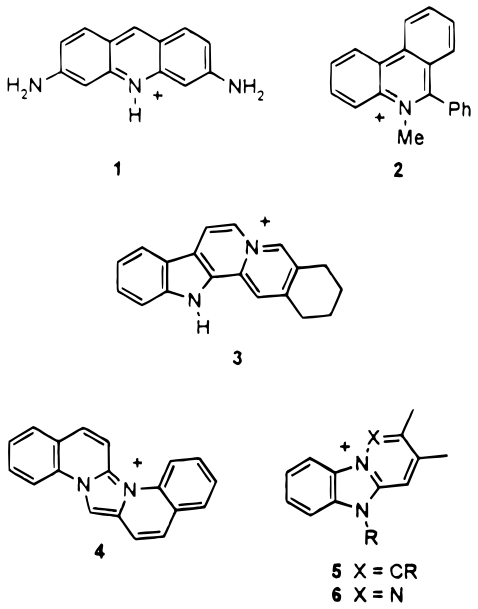

Figure 1.

In a recent communication[6] we reported our initial results on the DNA binding properties of new pyrido[1,2-*a*]- and pyridazino[1,6-*a*]benzimidazolium monomers **5** and **6**. Full details of the synthesis, simple chemical transformations, DNA-binding properties, and molecular modeling studies are reported herein.

Computational chemistry has proved to be of great benefit in understanding the determinants of specificity involved in the recognition process[7,8] and can be of further help in the design of new compounds with tailor-made binding properties. *Ab initio* molecular orbital methods have been used to calculate the molecular electrostatic potentials of some selected compounds and to assign point charges to their constituent atoms. In order to rationally modify these chromophores, and to produce bis-intercalating agents, it was essential to gain insight into the principles that dictate binding orientation. To achieve this, molecular modeling and molecular dynamics techniques were employed to explore the more stable chromophore−DNA complexes.

Computational Methods

Molecules **6a**,**d**−**g**,**i**,**n**,**o** were model-built in Insight-II[9] using standard geometries and were fully optimized by means of the *ab initio* quantum mechanical program Gaussian 92[10] and the 3-21G basis set. Single point calculations, using the larger

[†] Departamento de Química Orgánica.
[‡] Departamento de Química-Física.
[§] Departamento de Farmacología.
[⊗] Abstract published in *Advance ACS Abstracts,* July 15, 1997.

(1) Krugh, T. R. *Curr. Opin. Struct. Biol.* **1994**, *4*, 351.
(2) Waring, M. J.; *J. Mol. Biol.* **1970**, *54*, 247.
(3) Recent contributions from us: (a) Molina, A.; Vaquero, J. J.; García-Navío, J. L.; Alvarez-Builla, J.; de Pascual-Teresa, B.; Gago, F.; Rodrigo, M. M.; Ballesteros, M. *J. Org. Chem.* **1996**, *61*, 5587. (b) Molina, A.; Vaquero, J. J.; García-Navío, J. L.; Alvarez-Builla, J.; Rodrigo, M. M.; Castaño, O.; de Andrés, J. L. *Bioorg. Med. Chem. Lett.* **1996**, *6*, 1453.
(4) Caprasse, M.; Houssier, C. *Biochimie* **1984**, *66*, 31.
(5) Feigon, J.; Denny, W. A.; Leupin, W.; Dearns, D. V. *J. Med. Chem.* **1984**, *27*, 450.
(6) Pastor, J.; Siro, J. G.; García-Navio, J. L.; Vaquero, J. J.; Rodrigo, M. M.; Ballesteros, M.; Alvarez-Builla, J. *Bioorg. Med. Chem. Lett.* **1995**, *5*, 3043.
(7) Gallego, J.; Luque, F. J.; Orozco, M.; Burgos, C.; Alvarez-Builla, J.; Rodrigo, M. M.; Gago, F. *J. Med. Chem.* **1994**, *37*, 1602.
(8) Pascual Teresa, B.; Gallego, J; Ortiz, A. R.; Gago, F. *J. Med. Chem.* **1996**, *39*, 4810.
(9) Insight II, version 2.2.0 (1994), Biosym Technologies Inc., 9685 Scranton Road, San Diego, CA 92121.

S0022-3263(96)02055-5 CCC: $14.00

6-31G* basis set on the optimized RHF/3-21G geometries, were then carried out in order to calculate point charges that could accurately reproduce the molecular electrostatic potential.[11] The AMBER[12] all-atom force field parameters were used for the DNA dimers. Covalent parameters for the chromophores were derived, by analogy or through interpolation,[13] from those already present in the AMBER database. Torsional parameters for the methyl carboxylate group (compound **6g**) were determined by a combination of molecular mechanical and quantum mechanical calculations[14] (Supporting Information).

The complex of ellipticine with 5-iodocytidylyl-(3′-5′)-guanosine[15] was retrieved from the Cambridge Structural Database (ref EICGUA) and used as a template for modeling three different DNA intercalation sites: $d(CG)_2$, $d(GC)_2$, and $d(CC)_2$. Intercalated complexes of the simplest chromophore **6o** and each of these dinucleotide steps (hereafter referred to as CpG, GpC, and CpC) were built. For each complex, four different orientations of the chromophore are possible relative to the base pairs that make up the intercalation site (Figure 2). For the symmetrical sequences (*i.e.* CpG and GpC), orientations a and c, having the methyl group in the minor groove, and orientations b and d, having the methyl group in the major groove, are equivalent. In order to achieve electrical neutrality in the modeled complexes, one counterion resembling a hydrated sodium ion was placed in the bisector of the phosphate group located farther from the positive charge of the ligand.

We think this modeling strategy is fundamental if bis-intercalators are to be designed rationally, since the preferred orientation of the chromophore at the intercalation site may largely determine the location of the spacer in the corresponding bis-intercalator−DNA complex.[8]

The initial complexes were refined by performing 5000 steps of steepest descent energy minimization in a continuum medium of relative permittivity $\epsilon = 4r_{ij}$ using a cut-off of 10 Å for the nonbonded interactions. The systems were then subjected to molecular dynamics simulations in which the temperature was weakly coupled to a thermal bath[16] with a relaxation time of 0.1 ps. In a 5 ps heating phase, the temperature was raised to 300 K in steps of 10 K over 0.1-ps blocks, and the velocities were reassigned according to a Maxwell−Boltzmann distribution at each new temperature. This was followed by an equilibration phase of 15 ps at 300 K, in which the velocities were reassigned in the same way every 0.2 ps during the first 5 ps, and by an 80-ps sampling period, during which system coordinates were saved every 0.2 ps. The time step used was 1 fs in the heating period and 2 fs during the rest of the simulations. All bonds involving hydrogens were constrained to their equilibrium values by means of the SHAKE algorithm,[17] and the lists of nonbonded pairs were updated every 25 steps. For the initial 30 ps, selected sugar−phosphate backbone atoms were restrained to their reference positions in cartesian space by means of a harmonic force constant of 10 kcal mol^{-1} $Å^{-2}$. For the duration of the simulations all possible hydrogen bonds between DNA bases were restrained by use of harmonic force constants of 50 kcal mol^{-1} $Å^{-2}$ and 50 kcal mol^{-1} rad^{-2} for distances and angles, respectively.

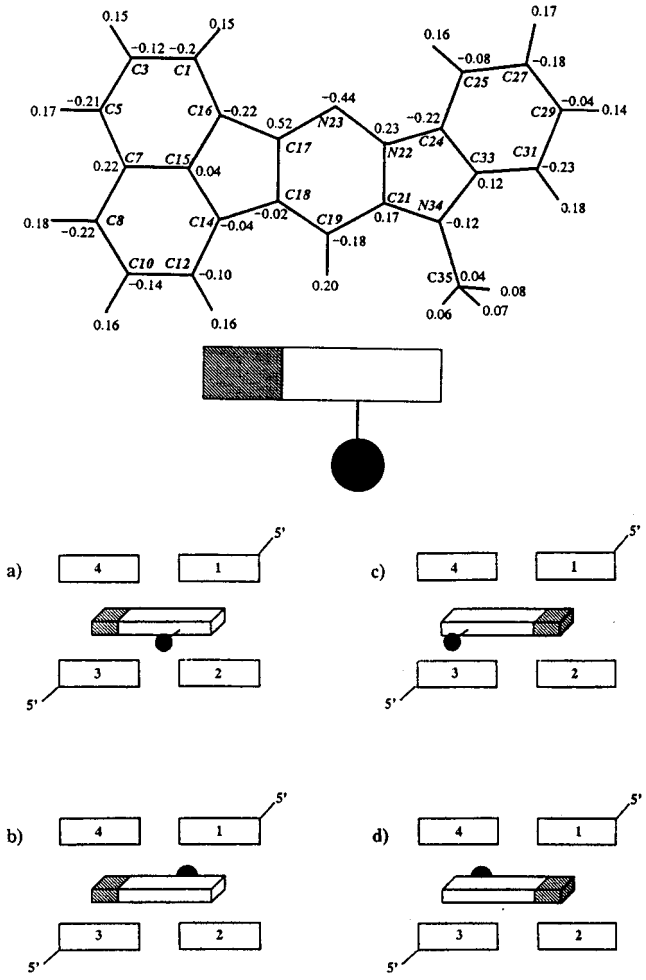

Figure 2. Top: Chemical structure of chromophore **6o** showing atom labels and point charges. Bottom: Schematic representations of **6o** and the four possible complexes it can form with dinucleotides CpG (C1,G2,C3,G4), GpC (G1,C2,G3,C4), and CpC (C1,C2,G3,C4).

Scheme 1

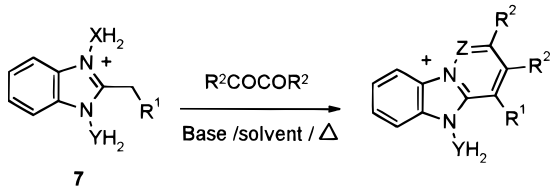

7

5 Z = C-H or C-CO_2Et
6 Z = N

DNA−ligand interaction energies were monitored and analyzed using the 400 coordinate sets saved during the last 80 ps of the molecular dynamics simulations. The energy analyses were performed using a dielectric constant of 1 for the electrostatic interactions and a cut-off distance of 10 Å. The energy contributions to the stacking interactions were calculated between the chromophore and the nucleobases using the deoxyribose C1′ atoms as buffers in order to achieve electrical neutrality.[8,18] Data smoothing for plotting purposes was accomplished by means of routine SMOOFT.[19]

Results and Discussion

Synthesis of DNA Chromophores. The new chromophoric structures **5** and **6** were straightforwardly

(10) Gaussian 92, Revision D.2, Frisch, M. J.; Trucks, G. W.; Head-Gordon, M.; Gill, P. M. W.; Wong, M. W.; Foresman, J. B.; Johnson, G.; Schlegel, H. B.; Robb, M. A.; Replogle, E. S.; Gomperts, R.; Andres, J. L.; Raghavachari, K.; Binkley, J. S.; González, C.; Martin, R. L.; Fox, D. J.; Defrees, D. J.; Baker, J.; Stewart; J. J. P.; Pople, J. A. Gaussian, Inc., Pittsburgh, PA, 1992.
(11) Besler, B. H.; Mertz, K. M., Jr.; Kollman, P. A. *J. Comput. Chem.* **1990**, *11*, 431.
(12) Pearlman, D. A.; Case, D. A.; Caldwell, J.; Seibel, G.; Singh, U. C.; Weiner, P.; Kollman, P. A. AMBER version 4.0 1991. Department of Pharmaceutical Chemistry, University of California, San Francisco.
(13) Weiner, S. J.; Kollman, P. A.; Nguyen, D. T.; Case, D. A. *J. Comput. Chem.* **1986**, *7*, 230.
(14) Hopfinger, A. J.; Pearlstein, R. A. *J. Comput. Chem.* **1984**, *5*, 486.
(15) Jain, S. C.; Bhandary, K. K.; Sobell. H. M. *J. Mol. Biol.* **1979,** *135*, 813
(16) Berendsen, H. J. C.; Postma, J. P. M.; Van Gunsteren, W. F.; DiNola, A.; Haak, J. R. *J. Chem. Phys.* **1984**, *81*, 3684.
(17) Ryckaert, J. P.; Ciccoti, G.; Berendsen, H. J. C. *J. Comput. Phys.* **1977**, *23*, 327.
(18) Gallego, J.; Ortiz, A. R.; Gago, F. *J. Med. Chem.* **1993**, *36*, 1548.
(19) Press, W. H.; Flannery, B. P.; Teukolsky, S. A.; Vetterling, W. T. In *Numerical Recipes*; Cambridge University Press: Cambridge, U.K., 1989.

Table 1. New Benzimidazolium Salts 7

compd[a]	X	Y	R^1	yield (%)	mp (°C)	compd[a]	X	Y	R^1	yield (%)	mp (°C)
7a	C-CO_2Et	CPh	H	82	240−243	**7h**	N	CC_6H_4-*p*-CO_2Me	H	90	202−203
7b	C-CO_2Et	CCO_2Et	H	89	249−250	**7i**	N	N	H	89	236−237
7c	N	CPh	H	86	200−202	**7j**	N	$CCH_2NHCOMe$	H	75	170−171
7d	N	CPh	Ph	84	206−208	**7k**	N	CC≡CH	H	94	192−193
7e	N	CCO_2Et	H	89	210−212	**7l**	N	$C(CH_2)_2C{\equiv}CH$	H	88	183−184
7f	N	CCH_2CO_2Et	H	87	131−132	**7m**	N	$CCONHCH_2C{\equiv}CH$	H	96	225−227
7g	N	$C(CH_2)_2CO_2Et$	H	79	106−107						

[a] Compounds **7a** and **7b** as bromides and the rest as mesitylenesufonates.

Table 2. New Pyrido[1,2-*a*] and Pyridazino[1,6-*a*]benzimidazolium Salts 5 and 6

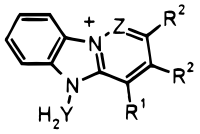

compd[a]	Z	Y	R^1	R^2	R^2	mp (°C)	yield (%)
5a	CCO_2Et	CPh	H	NPDL[b]		254−255	75
5b	CH	CPh	H	DPDL[c]		310−311	98
5c	CCO_2Et	CCO_2Et	H	NPDL		220−221	83
5d	CH	CCO_2Et	H	DPDL		278−279	56
5e	CCO_2Et	CCO_2H	H	NPDL		233−235	87
6a	N	CPh	H	NPDL		269−270	73
6b	N	CPh	Ph	NPDL		275−276	88
6c	N	CCO_2Et	H	NPDL		240−241	93
6d	N	CCO_2Et	H	Me	Me	140−142	82
6e	N	CCH_2CO_2Et	H	NPDL		214−215	83
6f	N	$C(CH_2)_2CO_2Et$	H	NPDL		236−237	82
6g	N	CC_6H_4-*p*-CO_2Me	H	NPDL		286−287	78
6h	N	N	H	NPDL		248−249	80
6i	N	$CCH_2NHCOMe$	H	NPDL		338−339	76
6j	N	CC≡CH	H	NPDL		273−274	81
6k	N	$C(CH_2)_2C{\equiv}CH$	H	NPDL		223−224	86
6l	N	$CCONHCH_2C{\equiv}CH$	H	NPDL		255−256	88
6m	N	$CCONHCH_2CH_2CH_3$	H	NPDL		164−166	78
6n	N	$CCONH(CH_2)_2NH_2$	H	NPDL		193−194	84

[a] Compounds **5** as bromides and mesitylenesufonates for salts **6**. [b] Naphathalene-1,8-diyl. [c] Biphenyl-*o*,*o*′-diyl.

obtained from the 1,3-disubstituted 2-alkylbenzimidazolium salts **7** (Scheme 1). Three different functionality types were introduced onto the indole-type nitrogen of the benzimidazole nucleus in order to facilitate access to bis-salts with linker chains of appropriate nature. Thus, compounds **7e**−**g** (X = N, Y = $C(CH_2)_nCO_2Et$, n = 0, 1, 2) and **7h** (X = N, Y = CC_6H_4-*p*-CO_2Me) bearing alkoxycarbonyl side chains were synthesized to allow us to study the influence of the position of the carboxy group in the linker chains. The acetamido salt **7j** (X = N, Y = $CCH_2NHCOCH_3$), with a reverse amido functionality was designed for comparison with products derived from **7g**, and, finally, the acetylenic group in salts **7k**,**l** (X = N, Y = $C(CH_2)_nC{\equiv}CH$, n = 0, 2) and **7m** (X = N, Y = $CCONHCH_2C{\equiv}CH$) were considered so as to study semirigid linkers when transformed into 1,3-diyne derivatives.

Basic condensation (dry sodium acetate as base, acetone as solvent, and refluxing) of benzimidazolium salts **7** with 1,2-diketones, aliphatic such as 2,3-butanedione or *o*-quinones as 1,2-acenaphthenequinone or 9,10-phenanthrenequinone, yielded pyrido[1,2-*a*] and pyridazino[1,6-*a*]benzimidazolium salts **5a**−**d**[20] and **6a**−**l**, respectively (Table 2). When one of the substituents on the nitrogen atoms in the benzimidazolium salts was an amino group, such as in **7e** (Z = N, Y = CCO_2Et), the condensation took place regioselectively to produce the pyridazino derivative **6c** (X = N, Y = CCO_2Et).

It has been pointed out that the presence of amino or amido funtionalities usually increases the ligand's DNA binding affinity.[21] Since most of the salts prepared

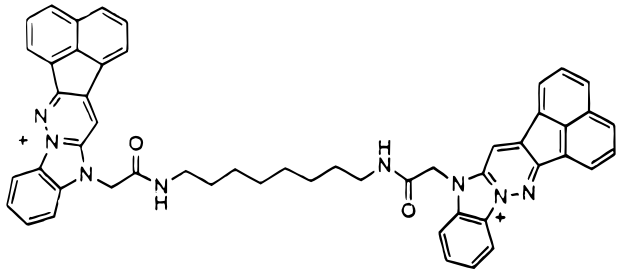

Figure 3.

contained an ethoxycarbonyl group, it seemed of interest to transform it into an amido group. Treatment of the (ethoxycarbonyl)methyl salt **6c** with simple amines such as *n*-propylamine produced the corresponding amide **6m,** although the amine itself had to be employed as solvent in order to achieve good yields. A similar reaction with 1,2-diaminoethane gave the monoamide **6n** (the best results were obtained using a 10 molar excess of diamine in refluxing acetonitrile). These kind of bifunctional

(20) It has ben previously reported, Westphal O., Jahn K., Heffe W. *Arch. Pharm.* **1961**, *294*, 37, that when 1-[(ethoxycarbonyl)methyl]-2-methylpyridinium bromide reacted with symmetrically substituted 1,2-diketones, except for 1,2-acenaphthenequinone, produced the corresponding quinolizinium bromides with loss of the ester group as the result of the *in situ* hydrolisis and descarboxylation of it. We have observed similar results with another related azinium salts; see Santiesteban, I.; Siro, J. G.; Vaquero, J. J.; García-Navío, J. L.; Alvarez-Builla, J.; Castaño, O.; Andrés, J. L. *J. Org. Chem.* **1995**, *60*, 5667 and references cited therein.

(21) Wakelin, L. P. G.; Waring, M. J. *Mol. Pharmacol.* **1974**, *10*, 544.

Table 3. Physical Properties and DNA Binding Properties and Cytotoxicity of Representative Examples of the Newly Described Products

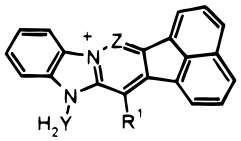

compd	Z	Y	R^1	K_{app}[a]	n[b]	visc[c]	IC_{50}[d]
5a	CCO_2Et	CPh	H	6.93	3.89	–	2.12
5c	CCO_2Et	CCO_2Et	H	0.93	3.88	–	1.80
6a	N	CPh	H	3.72	3.04	–	1.52
6b	N	CPh	Ph	0.29	3.22	–	3.67
6c	N	CCO_2Et	H	–	–	–	54.4
6e	N	CCH_2CO_2Et	H	0.69	3.87	0.85 ± 0.04	–
6f	N	$C(CH_2)_2CO_2Et$	H	0.44	3.38	0.74 ± 0.08	–
6g	N	CC_6H_4-*p*-CO_2Me	H	11.5	4.26	0.72 ± 0.15	24
6h	N	N	H	–	–	–	37
6i	N	$CCH_2NHCOMe$	H	0.34	4.14	0.64 ± 0.14	–
6j	N	CC≡CH	H	0.33	4.11	$1.04 + 0.08$	–
6k	N	$C(CH_2)_2C{\equiv}CH$	H	0.48	4.07	$1.09 + 0.08$	–
6l	N	$CCONHCH_2C{\equiv}CH$	H	1.58	4.95	$1.00 + 0.06$	–
6m	N	$CCONHCH_2CH_2CH_3$	H	0.34	4.14	0.77 ± 0.10	–
6n	N	$CCONH(CH_2)_2NH_2$	H	1.84	3.16	–	>100
6o[e]	N	CH	H	3.50	3.70	0.85 ± 0.15	3.70

[a] Apparent binding constants ($\times 10^5$ M^{-1}) of the compounds for calf thymus DNA. [b] Number of nucleotides per bound drug molecule. [c] Slope of the line representing the relative increase in DNA contour length (L/L_o) vs drug/nucleotide ratio (standard deviation of slope), by using the same buffer. [d] Dose (in μM) which inhibits growth of colon carcinoma HT-29 cells by half, as reported in ref 29. [e] Described in ref 25.

derivatives with free terminal amino and amido groups on the side chain are of interest because both groups could in principle interact with one of the DNA grooves, and they could in addition be used as precursors for other derivatives such as bis-salts, as will be described in forthcoming papers. However, when the condensation was performed with longer aliphatic diamines such as 1,8-diaminooctane under the same conditions (excess diamine, and reflux), the bis-salt **8** (Figure 3) was obtained directly. The high molar ratio amine to heterocyclic salt **6c** should not explain the formation of the bis-salt, and it is more likely that the high insolubility produces its separation from the reaction mixture. A shorter chain diamine, 1,4-diaminobutane, produced mixtures of the monoamide and the bis-salt products, which suggests that electrostatic repulsion between both cationic nuclei controls the formation of the bis-amide derivatives.

Interaction with DNA. The interaction of ligands with DNA results in a number of changes in the molecular properties of both species. These changes can be monitored by an array of biophysical and biochemical methods which have been divided into three different categories based on their simplicity and information content.[22] UV/vis-absorption spectroscopy represents one of the earliest methods used to follow the effects of ligand binding to DNA (first level tests). Binding usually results in hypochromism and shifts to longer wavelengths of the electronic transitions of the intercalated chromophore. A preliminary screening test for all the products described herein was carried out by comparing the UV/vis spectra of free and bound compounds (experiments were conducted at pH 7.5 in 50 mM Tris-HCl buffer [NaCl = 15 mM] containing 10 μM EDTA. Aliquots of a 1.2 mM DNA solution were added to a 0.2−0.6 mM solution of test compound). Using this routine test, derivatives bearing alkyl substituents on the pyridazino moiety were shown not to interact with DNA and were discarded for further modification. Three initial conclusions were then deduced from these experiments: (a) a minimum number of four linearly fused rings are needed to produce interaction with DNA in these systems, (b) steric hindrance arising from alkyl groups on the flat aromatic system is detrimental to binding, and (c) the presence of a flat polycyclic hydrocarbon moiety such as a naphthalene-1,8-diyl or a biphenyl-*o*,*o*'-diyl on R^2 appears to enhance the interaction.

DNA apparent affinity constants (K_{app}) were then measured on diluted solutions of selected salts by means of UV-vis titration with DNA, according to the procedure reported by Cory *et al.*[23] Table 3 shows values of K_{app} and *n*, the number of nucleotides per bound drug molecule. K_{app} values for most **5** and **6** salts are roughly comparable and lie within the range commonly observed for most DNA intercalating agents.[24] Replacement of the methyl group on the imidazolium nitrogen of **6o** (Y = CH, Z = N)[25] ($K_{app} = 3.5 \times 10^5$ M^{-1}) with a benzylic moiety (3.7×10^5 M^{-1} for **6a**) did not modify the affinity, which was increased by introduction of a methyl carboxylate group at the *para* position (11.5×10^5 M^{-1} for **6g**). A benzyl substituent on the imidazolium nitrogen was actually more favorable than a (methoxycarbonyl)methyl for binding affinity in the pyrido series **5** (6.9×10^5 M^{-1} for **5a** *vs* 0.9×10^5 M^{-1} for **5c**). Unfortunately **6c** was too insoluble to obtain reliable data. Increased separation of the ester group from the ring system by incorporation of one, **6e**, or two, **6f**, methylene groups have little effect on the binding constants (0.7 and 0.4×10^5 M^{-1}, respectively). Attachment of the amide-containing side chains to the imidazolium nitrogen (**6i**,**l**−**n**) did not significantly modify the binding affinities. The bis-salt **8** was not soluble enough for reliable data to be obtained, and precipitation of partially soluble complexes occurred in various common buffers. The K_{app} values obtained for

(22) Long, E. C.; Barton, J. K. *Acc. Chem. Res.* **1990**, *23*, 271.

(23) Cory, M.; Tidwell, R. R.; Fairley, T. A. *J. Med. Chem.* **1992**, *35*, 431.

(24) Pindur, U.; Haber, M.; Sattler, K. *J. Chem. Ed.* **1993**, *70*, 263.

(25) Matia, M. P.; García-Navío, J. L.; Vaquero, J. J.; Alvarez-Builla, J. *Liebigs Ann. Chem.* **1992**, 777.

the binding of **6o** to poly[d(AT)] and poly[d(GC)] polynucleotides were 4.2 and 3.8 × 10^5 M^{-1}, respectively, which are of the same order of magnitude as those obtained for binding to calf thymus DNA. Although this could be taken as evidence of non-sequence-specific binding, no definite conclusions can be drawn at this stage[26] as different binding modes might coexist under these experimental conditions.[22]

The main evidence for intercalative binding is provided by observing conformational changes in the DNA following insertion of the chromophore between the base pairs.[27] Hydrodynamic methods sensitive to length changes, of which sedimentation and viscosimetry are the most commonly used techniques,[28] are among the most stringent assays for testing the binding mode of DNA interacting agents. Viscosimetric determinations, in particular, give a semiquantitative measure of length change. The slope of the line representing the relative increase in DNA contour length (L/L_o) *vs* the drug/nucleotide ratio can be reproducibly determined (Table 3) and provides a simple and theoretically sound means of distinguishing among various DNA binding modes. The values obtained for representative compounds reported herein are characteristic of intercalators. The lower slopes observed are due to the different buffers used in our experiments. Except in the case of the dialkyl derivative **6d,** for which no interaction with DNA was detected, the results are comparable to those reported for classical intercalators (slope = 1.11 ± 0.06 using ethidium bromide **2** as the reference) with slight differences depending on the nature of the substituents.

IC_{50} on colon carcinoma HT-29 has been determined[29] for some representative compounds, including those with higher binding constants to DNA, to prove that intercalators maintain inhibitory activity on whole cellular preparations.

Molecular Modeling. Figure 2 shows the atom-based charge distribution for **6o**, calculated at the 6-31G*\\3-21G level and fitted so as to reproduce the electrostatic potential of the molecule. A color-coded representation of the molecular electrostatic potential (data not shown) shows the most positive area of the chromophore on the pyridazino ring and around atoms C19, C21, C35, and C33. The least positive regions are found on the lone pair of atom N23 and on the π faces of the naphthalene moiety and the aromatic ring at the other end of the chromophore. This distinct charge distribution should favor a particular orientation of the chromophore relative to the highly polarized G:C base pairs, whose most negative region is found in the surroundings of N7 and O6 atoms of guanines.[30]

The whole set of DNA−**6o** complexes studied contains different arrangements of the same number of atoms and atom types and can thus be directly compared. The complex that consistently displayed the most negative potential energies and showed the lowest root-mean-square deviations with respect to the initial structure was that formed between the CpG sequence and orientation a of the chromophore. The influence of chromophore orientation on complex stabilization becomes apparent on comparing the intermolecular interaction energies in orientations a (= c) and b (= d) for the same CpG step (Figure 4). The greater stability of CpG_a over CpG_b is related to better van der Waals and electrostatic interactions. Interestingly, while the van der Waals term of the stacking interactions between the chromophore and the base-pairs that make up this intercalation site is virtually the same on either side (≈−19.5 kcal mol^{-1}), the electrostatic contribution to stacking is attractive with base-pair G2:C3 but repulsive with C1:G4 (Figure 5). This is due to the antiparallel arrangement of the two G:C pairs (Figure 6) which makes their respective dipole moments adopt opposite orientations.[8,18] Nevertheless, none of the complexes with CpC, in which the two G:C base-pairs adopt parallel orientations, were more stable than CpG_a, which highlights the importance of electrostatic interactions involving the π electron systems and particular bond moments in the selection of the most favorable configuration.[31]

Based on these results, the CpG_a orientation was used to model the complexes of CpG with **6a**,**d**−**g**,**i**,**n**, which were likewise subjected to energy refinement and

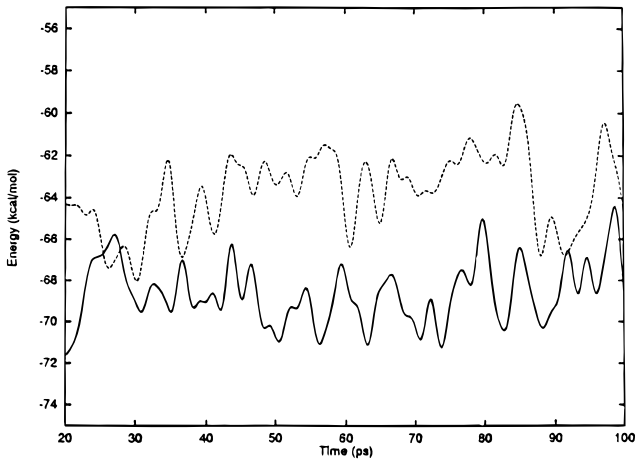

Figure 4. Time evolution of the total DNA−ligand interaction energy (kcal mol^{-1}) for the two possible complexes between CpG and **6o** along the molecular dynamics simulations. CpG_a (—), CpG_b (- - - - - -).

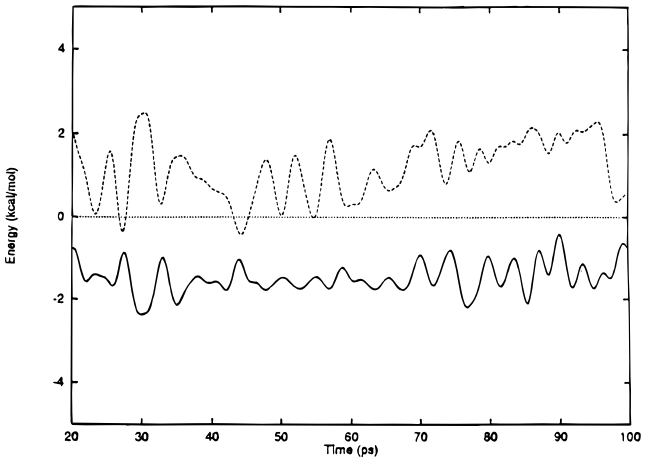

Figure 5. Time evolution of the electrostatic contribution to the stacking energy between chromophore **6o** in the CpG_a complex and either base-pair C1:G4 (- - - - - -) or G2:C3 (—).

(26) Leupin, W. In *Molecular Basis of Specificity in Nucleic Acid-Drug Interactions*; Pullman, B., Jortner, J., Eds.; Kluwer Academic Publishers: The Netherlands, 1990; p 579.
(27) Wakelin, L. P. G. *Med. Res. Rev.* **1986**, *6*, 275.
(28) Suh, D.; Chaires, J. B. *Bioorg. Med. Chem.* **1995**, *5*, 723.
(29) Braña, M. F.; Castellano, J. M.; Morán, M.; Pérez de Vega, M. J.; Romerdahl, C. A.; Quian, X.-D.; Bousquet, P.; Emling, F.; Schlick, E.; Keilhauer, G. *Anticancer Drug Res.* **1993**, *8*, 257.
(30) Lavery, R.; Pullman, B. *J. Biomol. Struct. Dyn.* **1985**, *2*, 1021.
(31) Bugg, C. E., Thomas, J. M., Sundaralingam, M., Rao, S. T. *Biopolymers* **1971**, *10*, 175.

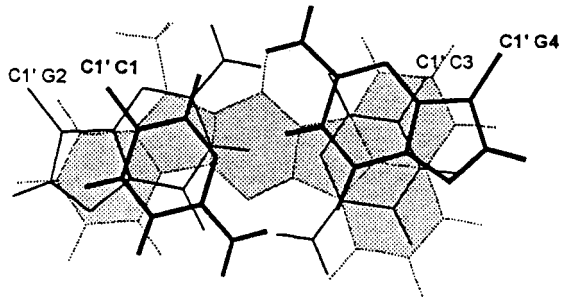

Figure 6. Schematic representation of the energy-optimized average structure of the preferred CpG_a:**6o** complex viewed along the normal of the best plane of the chromophore. In this orientation, the methyl group of the ligand lies in the minor groove of the DNA dimer, the quaternary nitrogen is situated between the N2 of G2 (thin lines) and the O2 of C1 (thick lines), and the naphthalene moiety is sandwiched between C3 (thin lines) and G4 (thick lines).

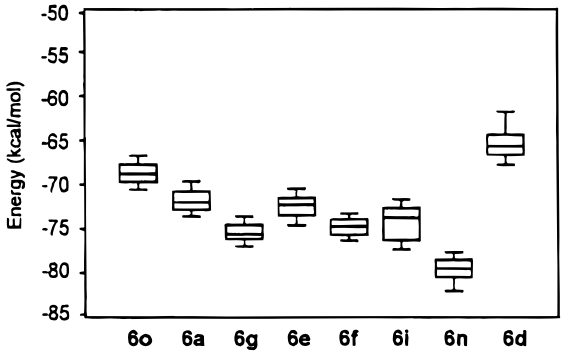

Figure 7. Box plot showing the median (line across the middle of each box), 25th and 75th percentiles (edges of the box), and 10th and 90th percentiles (lower and upper lines, respectively) of the total DNA−ligand interaction energies (kcal mol^{-1}) in the different CpG complexes in the a orientation during the 20−100 ps period of the molecular dynamics simulations.

molecular dynamics simulations. The time-weighted averages of the intermolecular interaction energy for each complex (Figure 7) show how the different interactions established between the various side chains and the minor groove modulate the calculated binding energies along the trajectories. The trends for the different substituents are in general agreement with the experimental affinity constants. Thus, the favorable effect of replacing a methyl by a benzyl group is easily discerned when **6o**, **6a**, and **6g** are compared, even though no specific binding site was found for the aromatic side chains of **6a** and **6g** within the minor groove of the CpG step. Pairwise comparisons of **6e** *vs* **6f** and **6i** *vs* **6n** are also consistent with the experimental data (Table 3). The low affinity for DNA of **6d**[6] is manifested both by the least favorable interaction energy among all the molecules studied (Figure 7) and by the fact that its orientation within the intercalation site was the most variable, as revealed by the large root-mean-square fluctuations from the initial structure (data not shown). Comparison of the whole set of molecules is hampered by the neglect of solvation/desolvation effects in the calculations and by the possible existence of additional nonintercalative binding modes in the experiments. It must also be born in mind that the simulation studies were perfomed on a particular dinucleotide step but no details of sequence-selective interactions are yet known for this class of compounds.

The larger surface area and greater polarizability of G:C base-pairs over A:T base-pairs[32] favor intercalation of planar chromophores into G/C-rich steps, of which CpG is usually preferred by most monointercalators,[33] with one notable exception in actinomycin D, which binds with high affinity to a GpC step.[34] The preference for CpG has been attributed to the lower energy required for unstacking this sequence relative to others[35] but could also be related to the fact that CpG is one of the most unwound steps in DNA.[36] When models of the two possible complexes of **6o** with $d(CG)_2$ were compared, a clear preference for one of the chromophore orientations was detected, in agreement with previous molecular mechanics studies in which the orientation of the chromophore relative to the base-pairs was systematically varied.[37] This highlights the interrelations among base-pair composition, 3′→5′ directionality, and chromophore orientation in the selection of a particular complex.[8] In the a conformation, the electrostatic component of the stacking interaction is attractive with respect to one of the base-pairs but repulsive with respect to the other one, given the antiparallel orientation of the G:C base-pairs that make up this intercalation step and the distinct charge distribution on the chromophore. One important consequence of this preferred orientation is that the substituents attached to the imidazolium ring will be located in the minor groove.

Validation of these theoretical models will have to await the results of additional studies with small oligonucleotides of known sequence currently underway, but the information already obtained is presently being used to design suitable spacers that will optimize their interactions with the minor groove of two contiguous CpG steps (Figure 8). A length of about 11 Å and an adequate disposition of complementary hydrogen bonding partners are some of the prerequisites that the new linking chains will have to fulfill.

Experimental Section[38]

Preparation of Benzimidazolium Salts. A. Quaternization with Ethyl Bromoacetate. Equivalent amounts (10 mmol) of the corresponding benzimidazole precursor and ethyl bromoacetate in dry acetone (30 mL) were refluxed for 4 h. The precipitate was collected and recrystallized from absolute ethanol as white prisms.

7a. Yield: 82%. Mp 240−243 °C. ^{1}H NMR (DMSO-d_6) 8.05−7.95 (m, 2 H); 7.65−7.60 (m, 2 H); 7.4−7.3 (m, 5H); 5.88 (s, 2 H); 5.64 (s, 2 H); 4.21 (q, 2 H, J = 7.2 Hz); 2.93 (s, 3 H); 1.22 (t, 3 H, J = 7.2 Hz). Anal. Calcd for $C_{19}H_{21}BrN_2O_2$: C, 58.62; H, 5,43; N, 7.19. Found: C, 58.80; H, 5.60; N, 7.01.

7b. Yield: 89%. Mp 249−250 °C. ^{1}H NMR (DMSO-d_6) 8.05−8.00 (m, 2 H); 7.65−7.60 (m, 2 H); 5.67 (s, 4H); 4.21 (q, 4H, J = 7.1Hz); 2.87 (s, 3 H); 1.24 (t, 6H, J = 7.2 Hz). Anal. Calcd for $C_{16}H_{21}N_2O_4Br$: C, 50.40; H, 4,49; N, 7.34. Found: C, 50.73; H, 4.26; N, 7.58.

(32) (a) Müller, W.; Crothers, D. M. *Eur. J. Biochem.* **1975**, *54*, 267. (b) Krugh, T. R.; Reinhardt, C. G. *J. Mol. Biol.* **1975**, *97*, 133.

(33) Krugh, T. R. *Curr. Opin. Struct. Biol.* **1994**, *4*, 351.

(34) (a) Sobell, H. M., Jain, S. C., Sakore, T. D.; Nordman, C. E. *Nature New Biol.* **1971**, *231*, 200. (b) Jain, S., C.; Sobell, H. M. *J. Mol. Biol.* **1972**, *68*, 1, c) Kamitori, S.; Takusagawa, F. *J. Mol. Biol.* **1992**, *225*, 445.

(35) (a) Ornstein, R. L.; Rein, R.; Breen, D. L.; MacElroy, R. D. *Biopolymers* **1978**, *17*, 2341. (b) Nuss, M. E.; Marsh, F. J.; Kollman, P. A. *J. Am. Chem. Soc.* **1979**, *101*, 825. (c) Aida, M.; Nagata, C. *Int. J. Quantum Chem.* **1986**, *29*, 1253.

(36) Gorin, A. A.; Zhurkin, V. B.; Olson, W. K. *J. Mol. Biol.* **1995**, *247*, 34.

(37) Pastor, M.; Pastor, J.; Alvarez-Builla, J. In *QSAR and Molecular Modelling: Concepts, Computational Tools and Biological Applications*; Sanz, J., Giraldo, J., Manaut, F., Eds.; Prous Science Publishers: Barcelona, 1995; p 592.

(38) For analytical intruments, standard spectral calibrations, and spectral data formats, see ref 3.

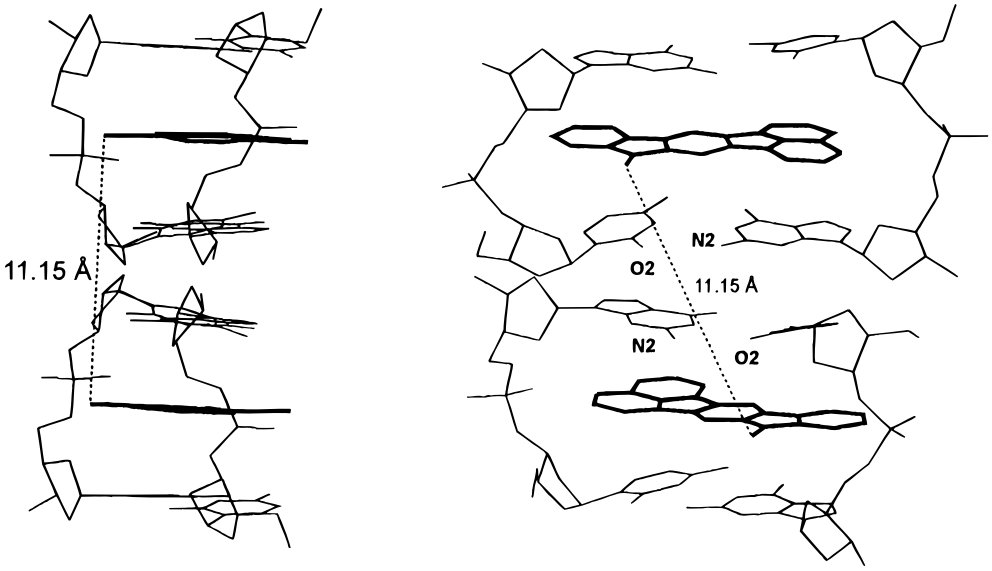

Figure 8. Side and front views of the putative 2:1 complex between **6o** (thick lines) and a $d(CGCG)_2$ tetramer (thin lines) displaying the approximate ideal distance for a linking chain that would permit bis-intercalation and the position of the hydrogen bond donor and acceptor atoms in the minor groove.

B. Amination with MSH. To a stirred solution of O-(mesitylenesulfonyl)hydroxylamine (MSH) (2.15 g, 10 mmol) in dichloromethane (20 mL) was added the corresponding benzimidazole (10 mmol) in the same solvent (20 mL) dropwise. The mixture was stirred at room temperature for 10 min. Diethyl ether (30 mL) was then added to precipitate the *N*-aminobenzimidazolium salts which were triturated with ether (3 × 5 mL) and recrystallized from absolute ethanol.

7c. Yield: 86%. Mp 200−202 °C (white powder). ^{1}H NMR (DMSO-d_6) 7.90 (d, 1H; J = 8.4 Hz); 7.87 (d, 1H; J = 8.4 Hz); 7.65−7.55 (m, 2 H); 7.4−7.3 (m, 5H); 6.63 (s, 2 H, NH_2); 5.76 (s, 2 H); 2.88 (s, 3 H). Anal. Calcd for $C_{24}H_{27}N_3O_3S$: C, 65.87; H, 6.21; N, 9.60. Found: C, 65.52; H, 5.95; N, 9.28.

7d. Yield: 84%. Mp 206−208 °C (white prisms). ^{1}H NMR (DMSO-d_6) 7.93 (d, 1H, J = 8.2 Hz); 7.7−7.6 (m, 2 H); 7.58 (d, 1H, J = 7.3 Hz); 7.3−7.2 (m, 8H); 7.05−6.95 (m, 2 H); 6.89 (s, 2 H, NH_2); 5.77 (s, 2 H); 4.84 (s, 2 H). Anal. Calcd for $C_{30}H_{31}N_3O_3S$: C, 70.14; H, 6.08; N, 8.18. Found: C, 69.91; H, 5.72; N, 7.95.

7e. Yield: 89%. Mp 210−212 °C (white powder). ^{1}H NMR (DMSO-d_6) 7.95 (d, 1H; J = 8.3 Hz); 7.85 (d, 1H; J = 7.3 Hz); 7.65−7.60 (m, 2 H); 6.77 (s, 2 H, NH_2); 5.57 (s, 2 H); 4.19 (q, 2 H; J = 7.3 Hz); 2.81 (s, 3 H); 1.22 (t, 3 H; J = 7.1 Hz). Anal. Calcd for $C_{21}H_{27}N_3O_5S$: C, 58.18; H, 6.28; N, 9.70. Found: C, 58.10; H, 6.15; N, 9.81.

7f. Yield: 87%. Mp 131−132 °C (white prisms). ^{1}H NMR (DMSO-d_6) 8.05−7.8 (m, 1 H); 7.85−7.8 (m, 1 H); 7.65−7.55 (m, 2 H); 6.77 (s, 2 H, NH_2); 4.67 (t, 2 H, J = 6.8 Hz); 4.02 (q, 2 H, J = 7.1 Hz); 2.97 (t, 2 H, J = 6.8 Hz); 2.88 (s, 3 H); 1.12 (t, 3 H; J = 7.1 Hz). Anal. Calcd for $C_{22}H_{29}N_3O_5S\cdot{}^3/_4H_2O$: C, 57.30; H, 6.65; N, 9.11. Found: C, 57.19; H, 6.31; N, 9.35.

7g. Yield: 79%. Mp 106−107 °C (white powder). ^{1}H NMR (DMSO-d_6) 8.0−7.95 (m, 1 H); 7.85−7.8 (m, 1 H); 7.65−7.6 (m, 2 H); 6.62 (s, 2 H, -NH_2); 4.46 (t, 2 H, J = 7.4 Hz); 3.99 (q, 2 H, J = 7.1 Hz); 2.84 (s, 3 H); 2.46 (t, 2 H, J = 7.9 Hz); 2.06 (m, 2 H); 1.12 (t, 3 H; J = 7.1 Hz). Anal. Calcd for $C_{23}H_{31}N_3O_5S\cdot{}^1/_2H_2O$: C, 58.70; H, 6.85; N, 8.93. Found: C, 58.74; H, 7.06; N, 9.26.

7h. Yield: 90%. Mp 202−203 °C (white powder). ^{1}H NMR (DMSO-d_6) 7.93 (d, 2 H; J = 8.1 Hz); 7.87(d, 1H; J = 8.0 Hz); 7.83 (d, 1H, J = 8.3 Hz); 7.63 (at, 1H; J = 7.7 Hz); 7.56 (at, 1H; J = 7.8 Hz); 7.43 (d, 2 H; J = 8.1 Hz); 6.70 (s, 2 H, -NH_2); 5.86 (s, 2 H); 3.81 (s, 3 H); 2.86 (s, 3 H). Anal. Calcd for: $C_{26}H_{29}N_3O_5S$: C, 63.01; H, 5.90; N, 8.48. Found: C, 63.12; H, 6.05; N, 8.33.

7i. Yield: 89%. Mp 236−237 °C (white prisms). ^{1}H NMR (DMSO-d_6) 7.85−7.80 (m, 2 H); 7.65−7.60 (m, 2 H); 6.64 (s, 2 H, NH_2); 2.78 (s, 3 H). Anal. Calcd for $C_{17}H_{22}N_4O_3S$: C, 56.33; H, 6.12; N, 15.47. Found: C, 56.20; H, 5.89; N, 15.18.

7j. Yield: 75%. Mp 170−171 °C (white prisms). ^{1}H NMR (DMSO-d_6) 7.94−7.91 (m, 2 H); 7.65−7.58 (m, 2 H); 6.71 (s, 2 H, -NH_2); 4.49 (ap.t, 2 H, J = 5.7 Hz); 3.49−3.45 (m, 2 H); 2.81 (s, 3 H); 1.60(s, 3 H). Anal. Calcd for $C_{21}H_{28}N_4O_4S$: C, 58.31; H, 6.53; N, 12.96. Found: C, 58.07; H, 6.60; N, 12.78.

7k. Yield: 94%. Mp 192−193 °C (white powder). ^{1}H NMR (DMSO-d_6) 8.00−7.95 (m, 1 H); 7.85−7.8 (m, 1 H); 7.65−7.55 (m, 2 H); 6.70 (s, 2 H, NH_2); 5.41 (d, 2 H, J = 2.4 Hz); 3.59 (t, 1 H, J = 2.4 Hz); 2.86 (s, 3 H). Anal. Calcd for $C_{20}H_{23}N_3O_3S$: C, 62.32; H, 6.01; N, 10.90. Found: C, 62.61; H, 6.31; N, 10.86.

7l. Yield: 88%. Mp 183−184 °C (white prisms). ^{1}H NMR (DMSO-d_6) 8.00−7.95 (m, 1 H); 7.85−7.8 (m, 1 H); 7.65−7.55 (m, 2 H); 6.70 (s, 2 H, -NH_2); 4.50 (d, 2 H, J = 7.1 Hz); 2.85 (s, 3 H); 2.83 (t, 1 H, J = 2.4 Hz); 2.28 (dt, 2 H, J = 7.2 and 2.7 Hz); 1.99 (m, 2 H). Anal. Calcd for $C_{22}H_{27}N_3O_3S$: C, 63.90; H, 6.58; N, 10.16. Found: C, 63.54; H, 6.79; N, 10.02.

7m. Yield: 96%. Mp 225−227 °C (white powder). ^{1}H NMR (DMSO-d_6) 9.05 (t, 1 H, J = 4.8 Hz): 7.85−7.8 (m, 1 H); 7.65−7.55 (m, 2 H); 6.77 (s, 2 H, NH_2); 5.27 (s, 2 H); 3.90 (dd, 2 H, J = 4.8 and 2.1 Hz); 3.32 (t, 1 H, J = 2.1 Hz); 2.78 (s, 3 H). Anal. Calcd for $C_{22}H_{26}N_4O_4S$: C, 59.71; H, 5.92; N, 12.66. Found: C, 59.76; H, 6.00; N, 12.27.

C. Basic Condensation. General Procedure. Equivalent amounts (10 mmol) of the benzimidazolium salts **7**, the dicarbonyl derivative, and anhydrous sodium acetate (0.82 g, 10 mmol) were suspended in dry acetone (10 mL). The mixture was refluxed for 6 h. The suspension was filtered and the solid washed with cold water (10 mL), Et_2O (2 × 10 mL), dried under vacuum, and recrystallized to give pure salts.

5a. Yield: 75%. Mp 254−255 °C (methanol, yellow powder). ^{1}H NMR (DMSO-d_6) 9.56 (s, 1 H); 8.62 (d, 1 H, J = 6.8 Hz); 8.31 (d, 1 H, J = 8.5 Hz); 8.24 (d, 1 H, J = 8.1 Hz); 8.1−7.9 (m, 6 H); 7.55 (d, 2 H; J = 6.6 Hz); 7.4−7.3 (m, 3 H); 6.15 (s, 2 H); 5.02 (q, 2 H; J = 6.8 Hz); 1.48 (t, 3 H; J = 6.9 Hz). Anal. Calcd for $C_{31}H_{23}BrN_2O_2\cdot{}^3/_2H_2O$: C, 66.19; H, 4.65; N, 4.98. Found: C, 66.50; H, 4.88; N, 4.85.

5b. Yield 98%. Mp 310−311 °C (methanol, yellow powder). ^{1}H NMR (DMSO-d_6) 10.89 (s, 1H); 9.57 (s, 1H); 9.11 (d, 2 H; J = 8.1 Hz); 8.75 (at, 2 H; J = 9.5 Hz); 8.0−7.7 (m, 8H); 7.46 (d, 2 H; J = 7.1 Hz); 7.4−7.3 (m, 3 H); 6.19 (s, 2 H). Anal. Calcd for $C_{30}H_{21}BrN_2\cdot{}^1/_2H_2O$: C, 72.29; H, 4.44; N, 5.62. Found: C, 71.94; H, 4.81; N, 5.34.

5c. Yield: 83%. Mp 220−221 °C (methanol, brown powder). ^{1}H NMR (DMSO-d_6) 9.47 (s, 1 H); 8.57 (d, 1 H, J = 7.1 Hz); 8.35 (dd, 1 H, J = 8.3 and 2.4 Hz); 8.25−8.2 (m, 2 H); 8.11 (dd, 1 H, J = 7.1 and 2.2 Hz); 8.0−7.9 (m, 4 H); 7.80 (at, 1 H,

J = 7.9 Hz); 5.94 (s, 2 H); 5.02 (q, 2 H, J = 7.1 Hz); 4.29 (q, 2 H; J = 7.1 Hz); 1.49 (t, 3 H; J = 7.1 Hz); 1.29 (t, 3 H; J = 7.1 Hz). Anal. Calcd for $C_{28}H_{23}BrN_2O_4$ C, 63.28; H, 4.36; N, 5.27. Found: C, 63.07; H, 4.56; N, 5.40.

5d. Yield: 50%. Mp 278−279 °C (methanol, brown powder). ^{1}H NMR (DMSO-d_6) 10.64 (s, 1 H); 9.32 (s, 1 H); 9.07 (d, 1 H, J = 7.8 Hz); 9.98 (d, 2 H, J = 7.3 Hz); 8.6−8.5 (m, 3 H); 8.10 (d, 1 H, J = 8.3 Hz); 7.95−7.6 (m, 8 H); 5.92 (s, 2 H); 4.25 (q, 2 H, J = 6.8 Hz); 1.28 (t, 3 H, J = 6.9 Hz). Anal. Calcd for $C_{27}H_{21}BrN_2O_2\cdot H_2O$: C, 64.42; H, 4.60; N, 5.56. Found: C, 64.47; H, 4.90; N, 5.42.

6a. Yield: 73%. Mp 269−270 °C (methanol, cream-colored powder). ^{1}H NMR (DMSO-d_6) 9.80 (s, 1 H); 8.6−8.55 (m, 3 H); 8.45−8.4 (m, 2 H); 8.16 (d, 1 H, J = 7.8 Hz); 8.05−8.0 (m, 2 H); 7.9−7.85 (m, 2 H); 7.58 (d, 2 H; J = 6.3 Hz); 7.42 (m, 3 H); 6.17 (s, 2 H). Anal. Calcd for $C_{36}H_{29}N_3O_3S$: C, 74.07; H, 5.00; N, 7.20. Found: C, 73.81; H, 4.90; N, 6.92.

6b. Yield: 88%. Mp 275−276 °C (methanol−acetone, yellow powder). ^{1}H NMR (DMSO-d_6) 8.69 (d, 2 H; J = 6.3 Hz); 8.43 (d 1 H, J = 7.8 Hz); 8.33 (d, 1 H, J = 8.3 Hz); 8.10 (at, 1 H, J = 7.6 Hz); 7.95−7.9 (m, 3 H); 7.7−7.6 (m, 6 H); 7.3−7.25 (m, 3 H); 7.05−7.0 (m, 2 H); 6.72 (d, 1 H, J = 7.3 Hz); 5.53 (s, 2 H). Anal. Calcd for $C_{42}H_{33}N_3O_3S$: C, 76.45; H, 5.04; N, 6.36. Found: C, 76.70; H, 5.05; N, 6.57.

6c. Yield: 93%. Mp 240−241 °C (methanol, yellow powder). ^{1}H NMR (DMSO-d_6) 9.64 (s, 1 H); 8.55−8.5 (m, 3 H); 8.4−8.35 (m, 2 H); 8.28 (d, 1 H, J = 8.1 Hz); 8.0−7.85 (m, 4 H); 5.96 (s 2 H); 4.27 (q, 2 H, J = 6.9 Hz); 1.28 (t, 3 H, J = 6.8 Hz). Anal. Calcd for $C_{33}H_{29}N_3O_5S$: C, 68.37; H, 5.04; N, 7.25. Found: C, 68.15; H, 5.26; N, 7.15.

6d. Yield: 82%. Mp 140−142 °C (methanol, brown powder). ^{1}H NMR (DMSO-d_6) 8.82 (s, 1 H); 8.41 (d, 1 H, J = 8.3 Hz); 8.19 (d, 1 H, J = 6.8 Hz); 7.9−7.75 (m, 2 H); 5.79 (s 2 H); 4.18 (q, 2 H, J = 6.3 Hz); 2.73 (s, 3 H); 2.59 (s, 3 H); 1.23 (t, 3 H, J = 6.5 Hz). Anal. Calcd for $C_{25}H_{29}N_3O_5S\cdot H_2O$: C, 59.86; H, 6.22; N, 8.37. Found: C, 60.19; H, 5.95; N, 8.34.

6e. Yield: 83% (methanol, yellow powder). Mp 214−215 °C. ^{1}H NMR (DMSO-d_6) 9.67 (s, 1 H); 8.60−8.50 (m, 3 H); 8.45−8.4 (m, 2 H); 8.34 (d, 1 H, J = 8.1 Hz); 8.05−8.0 (m, 2 H); 7.95 (at, 1 H, J = 7.6 Hz); 7.85 (at, 1 H, J = 7.7 Hz); 5.09 (t, 2 H, J = 6.9 Hz); 4.04 (q, 2 H, J = 7.1 Hz); 3.17 (t, 2 H, J = 6.7 Hz); 1.13 (t, 3 H, J = 7.1 Hz). Anal. Calcd for $C_{34}H_{31}N_3O_5S\cdot H_2O$: C, 66.75; H, 5.43; N, 6.87. Found: C, 66.81; H, 5.26; N, 7.15.

6f. Yield: 82%. Mp 236−237 °C (methanol, yellow powder). ^{1}H NMR (DMSO-d_6) 9.63 (s, 1 H); 8.61 (d, 1 H, J = 7.2 Hz); 8.57 (d, 1 H, J = 7.2 Hz); 8.54 (d, 1 H, J = 8.2 Hz); 8.44 (d, 1 H, J = 8.2 Hz); 8.41 (d, 1 H, J = 8.2 Hz); 8.31 (d, 1 H, J = 8.2 Hz); 8.44 (at, 2 H, J = 7.7 Hz); 7.97 (at, 1 H, J = 7.7 Hz); 7.86 (at, 1 H, J = 7.8 Hz); 4.90 (t, 2 H, J = 6.9 Hz); 3.97 (q, 2 H, J = 7.1 Hz); 2.56 (t, 2 H, J = 7.5 Hz); 2.3−2.25 (m, 2 H); 1.09 (t, 3 H, J = 7.1 Hz). Anal. Calcd for $C_{35}H_{33}N_3O_5S\cdot{}^1/_2H_2O$: C, 68.16; H, 5.56; N, 6.81. Found: C, 67.94; H, 5.67; N, 7.08.

6g. Yield: 78%. Mp 286−287 °C (methanol, yellow powder). ^{1}H NMR (DMSO-d_6) 9.74 (s, 1H); 8.6−8.5 (m, 3 H); 8.43 (dd, 2 H, J = 8.2 and 3.0 Hz); 8.1−8.0 (m, 3 H); 7.95 (d, 2 H, J = 8.1 Hz); 7.9−7.8 (m, 2 H); 7.65 (d, 2 H, J = 8.5 Hz); 6.25 (s, 2 H); 3.81 (s, 3 H). Anal. Calcd for $C_{38}H_{31}N_3O_5S$: C, 71.12; H, 4.87; N, 6.55. Found: C, 71.26; H, 5.03; N, 6.80.

6h. Yield: 80%. Mp 248−249 °C (methanol, yellow powder). ^{1}H NMR (DMSO-d_6) 9.39 (s, 1 H); 8.76 (d, 1 H, J = 7.1 Hz); 8.5−8.4 (m, 2 H); 8.4−8.3 (m, 2 H); 8.11 (d, 1 H, J = 8.1 Hz); 8.0−7.9 (m, 3 H); 7.84 (at, 1 H, J = 7.2 Hz); 7.07 (s, 2 H, NH_2). Anal. Calcd for $C_{29}H_{24}N_4O_3S$: C, 68.49; H, 4.76; N, 11.02. Found: C, 68.31; H, 4.63; N, 10.92.

6i. Yield: 90%. Mp 250−251 °C (methanol, yellow powder). ^{1}H NMR (DMSO-d_6) 9.77 (s, 1 H); 8.62 (d, 1 H, J = 7.3 Hz); 8.55 (d, 1 H, J = 7.3 Hz); 8.55 (at, 2 H, J = 7.6 Hz); 8.50−8.45 (bs, 1 H, NH); 8.40−8.35 (m, 2 H); 8.26 (d, 1 H, J = 8.5 Hz); 8.03 (at, 2 H, J = 7.6 Hz); 7.96 (at, 1 H, J = 7.4 Hz); 7.85 (at, 1 H, J = 7.8 Hz); 4.94 (bs, 2 H); 3.67 (bs, 2 H); 1.48 (s, 3 H). Anal. Calcd for $C_{33}H_{30}N_4O_4S\cdot H_2O$: C, 66.42; H, 5.41; N, 9.39. Found: C, 66.49; H, 5.06; N, 9.53.

6j. Yield: 81%. Mp 273−274 °C (methanol, yellow powder). ^{1}H NMR (DMSO-d_6) 9.76 (s, 1H); 8.63 (d, 1 H, J = 7.1 Hz); 8.6−8.55 (m, 2 H); 8.45−8.3 (m, 2 H); 8.32 (d, 1 H, J = 8.3 Hz); 8.05−7.9 (m, 3 H); 7.89 (at, 1 H, J = 7.7 Hz); 5.89 (d, 2 H, J = 2.2 Hz); 3.82 (t, 1 H, J = 2.2 Hz). Anal. Calcd for $C_{32}H_{25}N_3O_3S\cdot H_2O$: C, 69.93; H, 4.95; N, 7.64. Found: C, 69.97; H, 4.73; N, 7.83.

6k. Yield: 86%. Mp 223−225 °C (methanol, brown powder). ^{1}H NMR (DMSO-d_6) 9.69 (s, 1 H); 8.64 (d, 1 H, J = 7.1 Hz); 8.57 (d, 1 H, J = 7.1 Hz); 8.47 (d, 1 H, J = 8.3 Hz); 8.43 (d, 1 H, J = 8.3 Hz); 8.32 (d, 1 H, J = 8.2 Hz); 8.31 (d, 1 H, J = 8.3 Hz); 8.16 (at, 1 H, J = 7.7 Hz); 8.05 (at, 1 H, J = 7.7 Hz); 7.97 (at, 1 H, J = 7.7 Hz); 7.87 (at, 1 H, J = 7.8 Hz); 4.93 (t, 2 H, J = 6.6 Hz); 2.85 (bs, 1 H); 2.39 (at, 2 H, J = 7.3 Hz); 2.3−2.2 (m, 2 H). Anal. Calcd for $C_{34}H_{29}N_3O_3S\cdot{}^1/_2H_2O$: C, 70.69; H, 5.41; N, 7.27. Found: C, 70.45; H, 5.19; N, 7.18.

6l. Yield: 88%. Mp 255−256 °C (methanol, yellow powder). ^{1}H NMR (DMSO-d_6) 9.61 (s, 1 H); 9.9 (bs, 1 H); 8.56 (ad, 1 H, J = 7.8 Hz); 8.4−8.35 (m, 2 H); 8.17 (d, 1 H, J = 7.6 Hz); 8.05−9.0 (m, 2 H); 7.96 (at 1 H, J = 8.3 Hz); 7.87 (at 1 H, J = 7.8 Hz); 5.67 (s, 2 H); 3.99 (bs, 2 H); 3.21 (bs, 1 H). Anal. Calcd for $C_{34}H_{28}N_4O_4S$: C, 69.37; H, 4.79; N, 9.52. Found: C, 68.98; H, 4.76; N, 9.35.

6m. A solution of ethoxycarbonyl ester **6c** (0.5 mmol) and n-propylamine (5 mL) was refluxed for 1 h. Addition of diethyl ether precipitated the corresponding propyl amide which was purified by crystallization from methanol. Yield: 78%. Mp 164−166 °C (yellow powder). ^{1}H NMR (DMSO-d_6) 9.60 (s, 1 H); 8.67 (s, 1 H, NH); 8.55−8.50 (m, 3 H); 8.40 (d, 2 H, J = 8.1 Hz); 8.17 (d, 1 H, J = 8.3 Hz); 8.05−7.90 (m, 3 H) 7.86 (t, 1 H, J = 7.7 Hz); 5.62 (s, 2 H); 3.11 (q, 2 H, J = 5.6 Hz); 1.5−1.45 (m, 2 H); 0.85 (t, 3 H, J = 7.6 Hz). Anal. Calcd for $C_{34}H_{32}N_4O_4S\cdot{}^1/_2H_2O$: C, 67.86; H, 5.52; N, 9.31. Found: C, 67.66; H, 5.44; N, 9.57.

6n. A solution of ester **6c** (1 mmol) and ethylenediamine (0.6 g, 10 mmol) in dry acetonitrile (20 mL) was refluxed (18 h) in the presence of dry pyridine (0.79 g, 10 mmol). The precipitate was filtered and washed with acetonitrile (19 mL). Yield: 84%. mp 193−194 °C (yellow powder). ^{1}H NMR (DMSO-d_6) 9.60 (s, 1 H); 8.57 (bs, 1 H, NH); 8.55 (d, 3, J = 7.6 Hz); 8.40 (d, 2 H; J = 8.3 Hz); 8.19 (d, 1 H, J = 8.5 Hz); 8.05−7.85 (m, 4 H); 5.62 (s, 2 H); 3.16 (bs, 2 H); 2.62 (bs, 2 H). Anal. Calcd for $C_{33}H_{31}N_5O_4S$: C, 66.75; H, 5.26; N, 11.79. Found: C, 66.50; H, 5.51; N, 12.02.

8. A solution of ester **6c** (0.58 mg, 1 mmol), 1,8-diaminooctane (2.88 g, 20 mmol) and dry pyridine (0.79 g, 10 mmol) in dry acetonitrile (20 mL) was refluxed for 14 h. A precipitate was obtained which was isolated by filtration and then suspended in ethanol (10 mL) and acidified with concd HBr to yield the bis-amide salt as a yellowish solid (69%). Mp 205−206 °C (DMF). ^{1} H NMR (DMSO-d_6) 9.67 (s, 2 H); 8.6−8.5 (m, 8 H, 2 NH); 8.39 (at, 4 H; J = 7.2 Hz); 8.17 (d, 2 H, J = 8.5 Hz); 8.05−7.9 (m, 6 H); 7.86 (at, 2 H, J = 7.7 Hz); 5.60 (s, 4 H); 3.11 (aq, 4 H, J = 6.3 Hz); 1.45−1.4 (m, 4 H); 1.20 (bs, 8 H). Anal. Calcd for $C_{52}H_{44}N_8O_2Br_2$: C, 57.30; H, 5.27; N, 10.28. Found: C, 57.42; H, 5.16; N, 10.21.

Acknowledgment. We thank Dr. José Gallego for his help at the initial stages of the modeling work and Dr. Miguel Fernandez Braña (Knöll S.A.) for biological activity determinations. Financial support from the Comisión Interministerial de Ciencia y Tecnología (CICYT, project SAF-0280) and Comunidad Autónoma de Madrid (project AE00153/95) are gratefully acknowledged.

Supporting Information Available: Atom types for compounds **6a**,**d**−**g**,**i**,**n**,**o**, and AMBER parameters not included in the standard database (2 pages). This material is contained in libraries on microfiche, immediately follows this article in the microfilm version of the journal, and can be ordered from the ACS; see any current masthead page for ordering information. Cartesian coordinates of the energy-minimized time-averaged DNA-ligand complexes in PDB format are available from the authors on request (e-mail: ffgago@fisfar.alcala.es).

JO962055I